



HAL
open science

Sound emission from a 2-D thick turbulent boundary layer flow past an elongated cavity

Thangasivam Gandhi, Christophe Airiau, Azeddine Kourta, Thierry Poinso

► To cite this version:

Thangasivam Gandhi, Christophe Airiau, Azeddine Kourta, Thierry Poinso. Sound emission from a 2-D thick turbulent boundary layer flow past an elongated cavity. CFM 2009 - 19ème Congrès Français de Mécanique, Aug 2009, Marseille, France. hal-03378271

HAL Id: hal-03378271

<https://hal.science/hal-03378271>

Submitted on 14 Oct 2021

HAL is a multi-disciplinary open access archive for the deposit and dissemination of scientific research documents, whether they are published or not. The documents may come from teaching and research institutions in France or abroad, or from public or private research centers.

L'archive ouverte pluridisciplinaire **HAL**, est destinée au dépôt et à la diffusion de documents scientifiques de niveau recherche, publiés ou non, émanant des établissements d'enseignement et de recherche français ou étrangers, des laboratoires publics ou privés.

Sound emission from a 2-D thick turbulent boundary layer flow past an elongated cavity

THANGASIVAM GANDHI^a, CHRISTOPHE AIRIAU^a, AZEDDINE KOURTA^b, THIERRY POINSOT^a

a. Université de Toulouse, INPT, UPS, CNRS, IMFT, Allée du Pr Camille Soula, 31400, Toulouse, France

b. ESA/Institut PRISME, Polytech'Orléans, 8 Rue Leonard de Vinci, 45072, Orléans, France

Résumé :

L'aéroacoustique d'un écoulement généré par une couche limite turbulente épaisse affleurant une cavité est étudiée. L'apport énergétique important de la couche limite épaisse produit de forts cisaillement dans et en aval de la cavité qui modifient la dynamique de l'écoulement et la distribution des sources sonores. L'analyse du couplage aéroacoustique, par le modèle analogique de Curle, permet de caractériser les propagations sonores.

Abstract :

Aeroacoustics generated by a thick turbulent boundary layer in a cavity flow is studied. The thick boundary layer produces strong shear in the cavity and at the downstream of the cavity, it modifies the flow dynamics and the distribution of the sound sources. The analysis of aeroacoustics, using Curle's acoustic analogy model allows the characteristics of sound propagation

Keywords : cavity flow, thick turbulent boundary layer, Large Eddy Simulation, Aeroacoustics

1 Introduction

In a civil aircraft, the high lift systems and the landing gear are the most acoustically active airframe components. The flow in the cavities which are located on the aircraft surface is unsteady and, at typical landing speeds, may features large-width instabilities. The study of fluid flow over cavities is also relevant for a wide range of applications as car sunroof and turbo machinery.

Flow over the simple geometry of a cavity produces a rich variety of flow phenomena like separation, shear layer instabilities, multiple flow, resonant tones and acoustic instabilities with complex wave interactions. Rowley et al [1] portray that the cavity flow is a complicated dynamical system, it is comprised of only four elemental fluid dynamic processes : shear layer amplification of vortical disturbances, pressure wave generation through vortex-surface interaction, upstream propagation of acoustic waves receptivity at the upstream edge of the cavity and conversion of pressure waves into vorticity waves. The incompressible flow in and around axisymmetric cavities were studied experimentally by Gharib and Roshko [2] and it was found that the flow in a cavity is dependent on the Length to Depth ratio (L/D). An overview of various types of cavity flows and parameters that determines the character of the cavity flow are well presented in [3] and [4].

Study of turbulent cavity flows is concerned with the influence of incident turbulence on the hydrodynamic instabilities as well as the occurrence of self-sustained oscillations. Lin and Rockwell [5] observed that large-scale vertical structures related to the self-sustained oscillations with the incoming boundary layer was turbulent. Kang et al [6] found that the incoming turbulent boundary layer can give rise to the formation of large-scale vortical structures responsible for self-sustained oscillations.

This work concerns the study of 2-D rectangular cavities with an incoming thick boundary layer, in relevance to the reduction of noise and drag in many aerospace configurations. The cavity amplifies the kinetic energy modes contained in the incoming boundary layer structure. The unsteady flow interaction with the cavity walls generates aerodynamic noise. This mechanism differs from the traditional Rossiter instability mode, typical of cavities with a thin inflow boundary layer, and requires resolving the inflow outer layer eddies to capture their amplification across the cavity opening. A CFD model with Large Eddy Simulation approach and an acoustic analogy is used to resolve the flow disturbances that generate the aerodynamic noise by an interaction between fluid and the downstream corners and walls of the cavity. The generation of unsteady inflow data for spatially developing turbulent flows is one of the challenges. In the current work, for the moment, a mean turbulent boundary layer profile is imposed at the inlet of the domain. This work would be the initial step to study the aeroacoustics of three dimensional rectangular and cylindrical cavities with turbulent boundary layer.

2 Governing equations and numerical method

2.1 Governing equations

The compressible Navier-Stokes equations in Cartesian coordinates without body forces or external heat addition can be written as

$$\frac{\partial U}{\partial t} + \frac{\partial E_j}{\partial x_j} = \frac{\partial F_{ij}}{\partial x_j}$$

where $U = [\rho, \rho u_i, \rho E_t]^T$ is the state vector, $E_j = [\rho u_j, \rho u_i u_j + p \delta_{ij}, \rho E_t u_j + p u_j]^T$ are the inviscid fluxes, $F_{ij} = [0, \tau_{ij}, \tau_{ij} u_i - q_j]^T$ are the diffusive fluxes and the viscous stress tensor is $\tau_{ij} = \mu \left(\frac{\partial u_i}{\partial x_j} + \frac{\partial u_j}{\partial x_i} + \frac{2}{3} \frac{\partial u_k}{\partial x_k} \delta_{ij} \right)$,

where δ_{ij} is the Kronecker delta function. The heat flux from Fourier's heat law is given by $q_i = -\frac{c_p \mu}{Pr} \frac{\partial T}{\partial x_i}$ where c_p is the specific heat capacity at constant pressure, Pr is Prandtl number and $E_t = E + u_i u_i / 2$ is the total energy.

2.2 Numerical method – LES model

The parallel code AVBP from CERFACS, Toulouse, solves the laminar and turbulent compressible Navier-Stokes equations in two and three space dimensions. For turbulent flows, turbulence models are available. For prediction of unsteady turbulent flows, Direct Numerical Simulation (DNS) or Large Eddy Simulation (LES) are employed. The numerical schemes in AVBP are based on the cell-vertex method which naturally ensures high compactness. The main convective schemes are a finite volume Lax–Wendroff type scheme (LW) and a finite element two-step Taylor-Galerkin scheme (TTGC) [7]. These two schemes are respectively 2^{nd} and 3^{rd} order in time and space. The diffusive scheme is a typical 2^{nd} order compact scheme. In this work we typically use quadrangle elements for space discretization. Time integration is fully explicit to maximize accuracy. The derivation of the new governing equations is obtained by introducing operators to be applied to the set of compressible Navier-Stokes equations. Unclosed terms arise from these manipulations and need to be modeled for the problem to be solved. The operator in LES is a spatially localized time independent filter of given size, Δ , to be applied to a single realization of the studied flow. The unclosed terms in LES represents the physics associated with the small structures present in the flow. The LES predictions of complex turbulent flows are closer to the physics since large scale phenomena such as large vortex shedding and acoustic waves are embedded in the set of governing equations [8]. The filtered compressible Navier-Stokes equations exhibit sub-grid scale (SGS) tensors and vectors describing the interaction between the non-resolved and resolved motions. The influence of the SGS on the resolved motion is taken into account by a SGS model based on the introduction of a turbulent viscosity ν_t . The case presented here is simulated using LES–Smagorinsky

model $\nu_t = (C_S \Delta)^2 \sqrt{2 \widetilde{S}_{ij} \widetilde{S}_{ij}}$, where C_S is the model constant and \widetilde{S}_{ij} is the resolved strain rate tensor. Compressible flows are characterized by waves whose physics is to be respected in numerical simulations. Characteristic boundary conditions allow for the correct treatment of waves impinging on the boundary of the computational domain. Characteristic conditions for Euler equations were first derived by Thompson [9] and extended to the Navier-Stokes equations by Poinso and Lele [10]. To prevent the numerical oscillations in the region of high gradients, artificial viscosity is added. Schönfeld Lartigue Kaufmann sensor (SLK) [11] is used with values of 0.2 and 0.05 for the 2^{nd} and 4^{th} order respectively.

3 Aeroacoustics

Computational Aeroacoustics is to predict the sound radiated by turbulent flows, to identify the source of sound and to investigate strategies by which noise could be reduced. Computational Aeroacoustics combines the classical approaches of flow field computation with acoustics. The approaches such as experimental, analytical and numerical methods are used to investigate aeroacoustic sound sources. The direct computation of sound using DNS is restricted to low Reynolds numbers and very simple geometries. Hybrid method where the sound is obtained in a successive step, after having calculated the flow field is employed as found in Lighthill [12] where an analogy between the propagation of sound in an unsteady unbounded flow to that in a uniform medium at rest, generated by a distribution of quadrupole acoustic sources. In this analogy, Navier-Stokes equations are replaced by an inhomogeneous wave equation namely the Lighthill equation. The Lighthill analogy does not include the effect of solid boundaries in the flow, thus it considers only aerodynamically generated sound without solid body interaction. The formulation was extended by Curle [13] and Ffow Williams and Hawkins [14] to take into account the generation and the scattering mechanisms when solid bodies are present.

$$\frac{\partial^2 \rho}{\partial t^2} - a_\infty^2 \frac{\partial^2 \rho}{\partial x_i^2} = \frac{\partial^2 T_{ij}}{\partial x_i \partial x_j} \quad (1)$$

where $T_{ij} = \rho u_i u_j - \tau_{ij} + (p - a_\infty^2 \rho) \delta_{ij}$ is the Lighthill stress tensor and a_∞ is the speed of sound. The equation (1) includes all physics as no assumption is made in deriving it from the governing equations. An assumption is made that the equation is an inhomogeneous wave equation in an isotropic medium at rest and it becomes explicit when assuming $\rho \sim \rho_\infty$ in T_{ij} . The explicit form of the equation (1) can be solved analytically as

$$\rho(\mathbf{x}, t) - \rho_\infty = \frac{1}{4\pi a_\infty^2} \int_\infty \frac{1}{r} \frac{\partial^2 T_{ij}}{\partial x_i \partial x_j} dV(\mathbf{y}) \quad (2)$$

\mathbf{x} is the observer position, \mathbf{y} is the source position and $r = |\mathbf{x} - \mathbf{y}|$ is the distance between them. Curle [13] formulated an analogy for non-moving solid bodies using a general solution of equation (1)

$$\rho(\mathbf{x}, t) - \rho_\infty = \frac{1}{4\pi a_\infty^2} \int_V \frac{1}{r} \frac{\partial^2 T_{ij}}{\partial x_i \partial x_j} dV(\mathbf{y}) - \frac{1}{4\pi} \int_S \left(\frac{1}{r} \frac{\partial \rho}{\partial n} + \frac{1}{r^2} \frac{\partial r}{\partial n} \rho + \frac{1}{a_\infty r} \frac{\partial r}{\partial n} \frac{\partial \rho}{\partial \tau} \right) dS(\mathbf{y}) \quad (3)$$

where n is the surface normal pointing towards to fluid and $\tau = t - r/a_\infty$ is the retarded time, which is the time of the emission of a signal that reaches the observer location at time t . After handling the equation (3) with Green's function and considering the observer located in a region where the flow is isentropic, the final surface integral is a line integral along the cavity walls between $-b$ and $+b$, where b is the half cavity spanwise length, yielding

$$p(\mathbf{x}, t) - p_0 = \frac{1}{4\pi} \int_L l_i n_j \left[2 \arctan(b/r) \frac{\dot{p} \delta_{ij}}{a_\infty} + 2b \frac{p \delta_{ij}}{r^2} \right] dL(\mathbf{y}) \quad (4)$$

where l_i is an unit vector pointing from the source to the observer, \dot{p} is derivative of pressure with respect to time t [15] and [16]. At low Mach numbers, the surface integral term in the equation (3) is larger than the volume integral part, therefore in many cases the volume integral can be neglected. The time derivative of pressure is needed to compute the integrand term of the Curle expression and is calculated with a second order central difference scheme. The results presented in this work use equation (4), which takes into account the real half width (b) of the cavity. An acoustic code is developed at the partner institute Politecnico di Torino, Italy, to calculate the Sound Pressure Level (*SPL*).

4 Configuration

4.1 Test-case geometry and inflow condition

The flow is from left to right hand side. The domain extends between $0 \leq x/D \leq 25$ and $-1 \leq y/D \leq 20$. The computational domain extends to $5D$ and $16D$ upstream and downstream of the cavity leading and trailing edges, respectively. The dimensional variables which characterize the cavity flow [17] are L , D , free stream velocity U_∞ , momentum thickness θ , a_∞ , and kinematic viscosity ν_∞ . The role played by the momentum thickness θ at the leading edge of the cavity in the selection of modes is observed by Colonius et al [18]. The flow parameters relevant to the case in this work are given in the table 1.

L/D	U_∞	M_∞	Re_D	δ [mm]	θ [mm]	Re_θ	L/θ
4	40 m/s	0.117	27.37×10^3	19.08	1.857	1270	21.54

Table 1: Flow parameters.

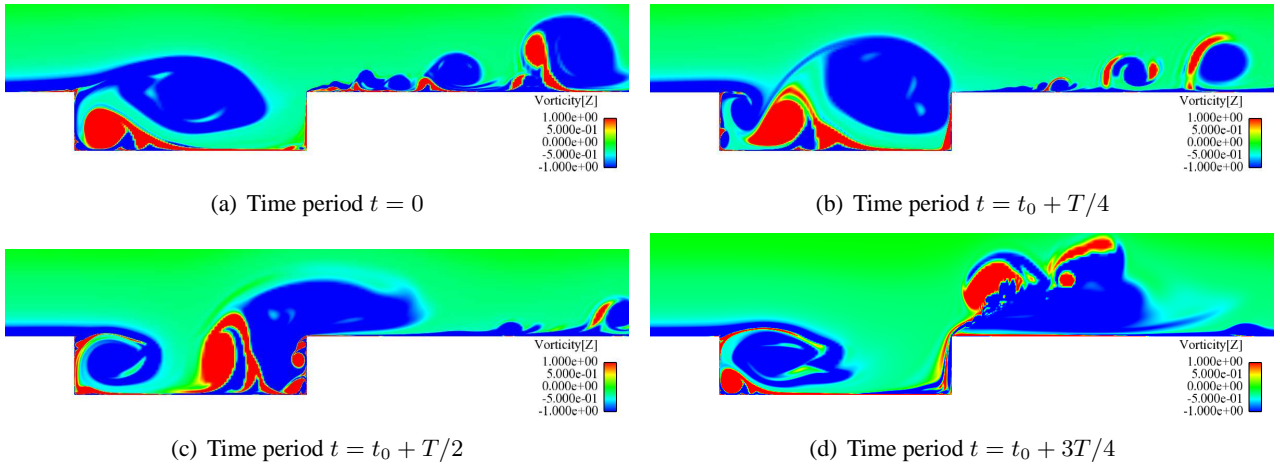
5 Starting flow condition

A power law boundary layer profile is imposed on the whole computational domain with the following flow state values : $P_0 = 101325 Pa$, $T_0 = 288.15 K$, $v_0 = 0 m/s$. A mean turbulent boundary layer profile is imposed at the inlet of the domain. At the inflow, $u = u_\infty$ and $\rho = \rho_\infty = 1.2 kg/m^3$ and at the outflow, pressure $P = 101325 Pa$ are imposed. The CFL value for this simulation is 0.7. The wall temperature is held constant and equal to the free stream value $T_\infty = 288.15 K$. Computations are performed in parallel on 16 to 64 nodes of an IBM-SP computers at IDRIS, Paris.

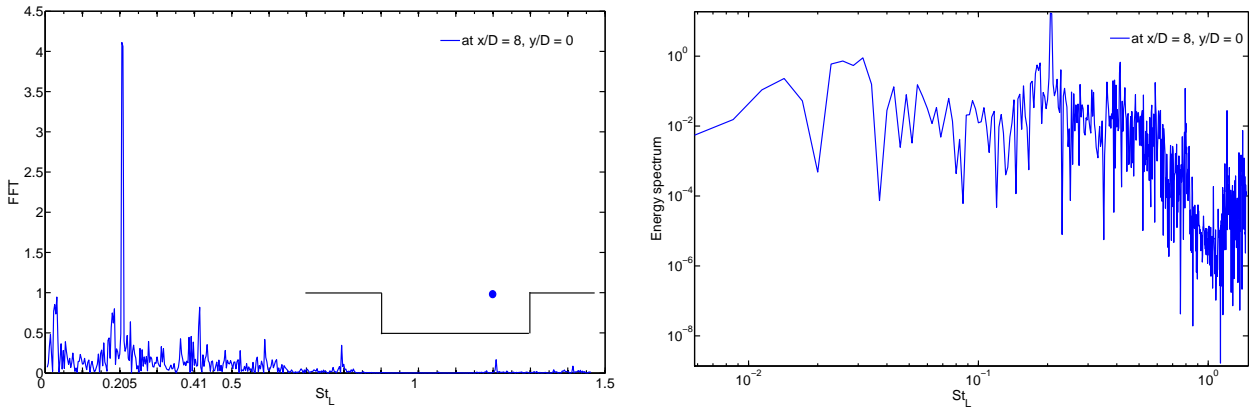
6 Results

6.1 Flow features

The incoming boundary layer behaves like a flat plate boundary layer which can be observed in the figure 3(a). Time averaged velocity profiles are plotted at $x/D = 2, 4$ and 5 . As shown in figure 1, we observe a wake mode observed for the above flow configuration. In the figure 1(a), a vortex is formed from the leading edge of the cavity and fills the cavity region and in the figure 1(b) the vortex detaches and impinges on the downstream

Figure 1: Instantaneous vorticity fields ω_z .

corner of the cavity. The flow above the cavity region is affected by the flow from the cavity. The free stream flow is periodically directed into the cavity. The spectrum calculated at point $[x/D, y/D] = [8, 0]$ is plotted in figure 2. The sampling time was $100 \leq T \leq 800$. Fast Fourier Transform (FFT) of velocity component in x -direction versus the Strouhal number (defined by $St_L = fL/U_\infty$) is shown in the figure 2(a). The fundamental frequency for this test case is $St_L = 0.205$, and all higher modes are harmonics of this fundamental frequency. The fundamental frequency St_L reported by Larsson et al [15] is 0.245 which is worth mentioning here. Colonius et al [19] found a fundamental frequency of $St_L = 0.248$. Figure 2(b) which represents an energy spectrum demonstrates the energy cascade where the peaks corresponding to the dominant oscillation frequency and its harmonic can be observed. At the locations $x/D = 6, 7$ and 8, mean stresses



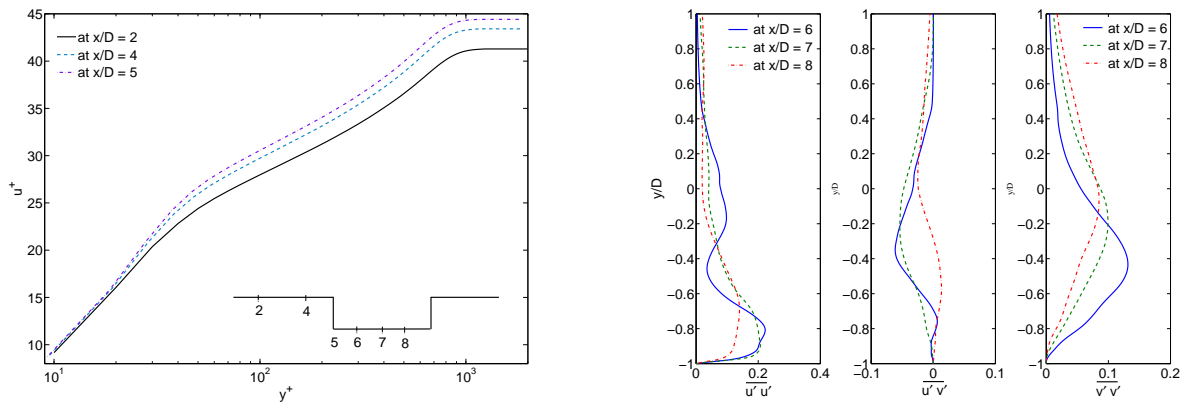
(a) FFT spectrum at $x/D = 8, y/D = 0$, sampling time $100 \leq T \leq 800, L/D = 4$ (b) Energy spectrum at $x/D = 8, y/D = 0$, sampling time $100 \leq T \leq 800, L/D = 4$

Figure 2: (a) FFT and (b) Energy spectra of velocity component in x -direction.

$\overline{u'u'}, \overline{u'v'}, \overline{v'v'}$ profiles are plotted and shown in the figure 3(b). The turbulent shear stress $\overline{u'v'}$ is directly linked with large eddies motion. So the anisotropic contribution to flow fluctuations is mostly distributed on the low frequency part of the spectrum. $\overline{u'u'}$ and $\overline{v'v'}$ may contribute more significantly to the high frequencies part.

6.2 Radiated Sound

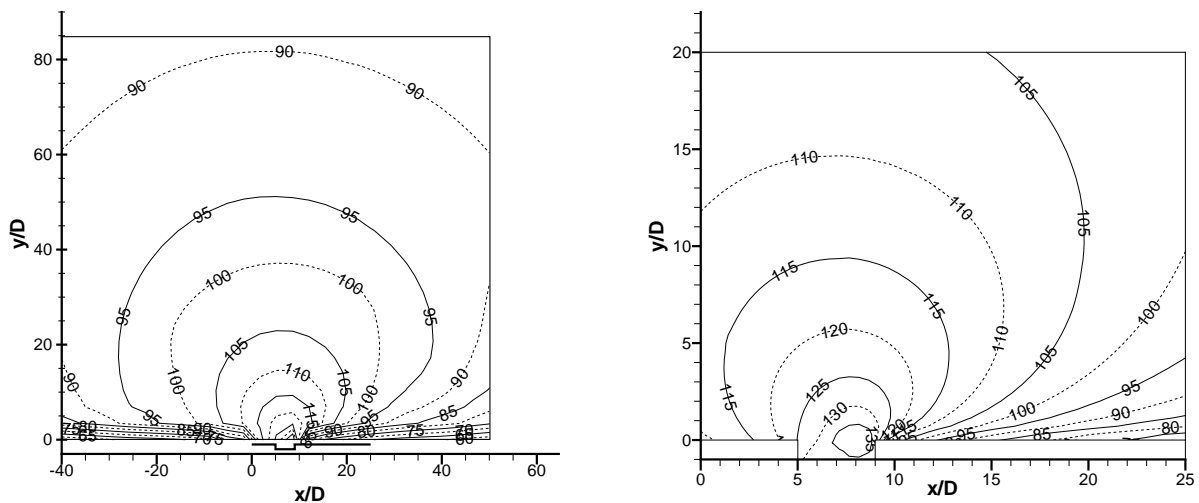
As mentioned in the section 6.1, the interaction of the vortex with the trailing edge of the cavity generates pressure waves which are radiated into the far field. These pressure waves are identified as aerodynamic noise. To determine the SPL using the acoustic analogy, two acoustic domains are generated. The first domain is of size $-40 \leq x/D \leq 50$ and $0 \leq y/D \leq 90$ (figure 4(a)) with 30×30 grid points and the second domain is of LES domain size $0 \leq x/D \leq 25$ and $-1 \leq y/D \leq 20$ (figure 4(b)) with 50×50 grid points. The intersection points of the grid represent the observers. SPL values are calculated for both domains. The figure 4 shows SPL iso-contours, $SPL = 20 \log(p_{rms})/p_{ref}$ above the enclosure of the cavity, where $p_{ref} = 20 \mu Pa$ and p_{rms} is the root mean square pressure fluctuation. The contour spacing is $\Delta SPL = 5 dB$ SPL iso-contours appear to be concentric about the trailing edge of the cavity, which confirms that the trailing edge is the main



(a) Time average velocity profiles in wall units at $x/D = 2, 4, 5$ (b) Mean stress profiles $\overline{u'u'}$, $\overline{u'v'}$ and $\overline{v'v'}$ at $x/D = 6, 7$ and 8

Figure 3: (a) Time average velocity profiles and (b) Mean Reynolds stress profile.

source of sound at the selected conditions. At the trailing edge of the cavity, the maximum value of SPL is found to be $135dB$ which confirms the louder flow. The direction of sound propagation appears uniform in this current case of low Mach number ($M = 0.117$) shallow cavity flow with turbulent incoming boundary layer. Similar qualitative concentric iso-contours are found by Haigermoser [16]. But Rowley et al [20] show the peak radiation to the far field occurs at an angle of about 135° from the downstream axis for the cavity $L/D = 2$ and Mach number $M = 0.6$. But in the present case, the directivity angle is not prominent. The discrepancy may be due to the low Mach number flow.



(a) Sound Pressure Level in the far field

(b) Sound Pressure Level in the LES computational domain

Figure 4: Sound Pressure Level.

7 Conclusions and Perspectives

In this work, the LES coupled with Curle’s acoustic analogy has been used to investigate the nature of cavity mechanism and sound generation. The incoming flow with a mean turbulent boundary layer profile at $Re_D = 27.37 \times 10^3$ over a two dimensional cavity with $L/D = 4$ was simulated. The main sources of sound in this low Mach number flow are the pressure fluctuations on the walls. In addition, the sources of the sound are large on the downstream cavity wall. The differences in the directivity of the sound propagation is certainly an interesting part which should be studied in the future. The next step could be studying the turbulent $2D$ and $3D$ cavity flow with the unsteady inflow data imposed at the inlet and analyzing the acoustics by including the volume integral part in acoustic analogy to improve the calculation of SPL values.

8 Acknowledgment

This research project has been supported by the AeroTraNet Marie Curie Early Stage Research Training Fellowship of the European Community's Sixth Framework Programme under contract number MEST CT 2005 020301. Thanks to Christian Haigermoser for the useful discussions. Thanks to DIASP, Politecnico di Torino for the acoustic code. We would like to thank the IDRIS, Paris of the CNRS for providing the computing facilities for performing our calculations.

References

- [1] Rowley C. W. and Williams D. R. Dynamics and control of high-Reynolds-number flow over open cavities. *Annual Review of Fluid Mechanics*, 38, 251–276, 2006.
- [2] Gharib M. and Roshko A. The effect of flow oscillations on cavity drag. *Journal of Fluid Mechanics*, 177, 501–530, 1987.
- [3] Rockwell D. and Naudascher E. Review-self-sustaining oscillations of flow past cavities. *Journal of Fluids Engineering*, 100, 152–165, 1978.
- [4] Rockwell D. and Naudascher E. Self-sustained oscillations of impinging free shear layer. *Annual Review of Fluid Mechanics*, 11, 67–94, 1979.
- [5] Lin J. C. and Rockwell D. Organized oscillations of initially turbulent flow past a cavity. *AIAA Journal*, 39(6), 1139–1151, 2001.
- [6] Kang W., Lee S. B., and Sung H. J. Self-sustained oscillations of turbulent flows over an open cavity. *Experiments in Fluids*, 45(4), 693–702, 2008.
- [7] Colin O. and Rudgyard M. Development of high-order Taylor-Galerkin schemes for LES. *Journal of Computational Physics*, 162, 2000.
- [8] Poinso T. and Veynante D. *Theoretical and Numerical Combustion*. R T Edwards, 2001.
- [9] Thompson K. W. Time dependent boundary conditions for hyperbolic systems. *Journal of Computational Physics*, 68, 1–24, 1987.
- [10] Poinso T. J. and Lele S. K. Boundary conditions for direct simulations of compressible viscous flows. *Journal of Computational Physics*, 101, 104–129, July 1992.
- [11] Colin O. *Simulation aux Grandes Echelles de la Combustion Turbulente Prémélangée dans les Statoréacteurs*. PhD thesis, Institut National Polytechnique de Toulouse, 2000.
- [12] Lighthill M. J. On sound generated aerodynamically: I. General Theory. *Proceedings of the Royal Society of London, Series A*, 211, 564–587, 1952.
- [13] Curle N. The influence of solid boundaries upon aerodynamic sound. *Proceedings of Royal Society of London, A23*, 505–514, 1955.
- [14] Ffowcs Williams J. E. and Hawkings D. L. Sound generation by turbulence and surfaces in arbitrary motion. *Philosophical Transactions of the Royal Society, A264(1151)*, 321–342, 1969.
- [15] Larsson J., Davidson L., Eriksson L.-E., and Olsson M. Aeroacoustic investigation of an open cavity at low Mach number. *AIAA*, 42(12), 2462–2473, 2004.
- [16] Haigermoser C. *Investigation of cavity flows using advanced optical methods*. PhD thesis, Politecnico di Torino, 2009.
- [17] Colonius T. An overview of simulation, modeling and active control of flow/acoustic resonance in open cavities. *AIAA paper*, 2001. 2001–0076.
- [18] Colonius T. and Lele S. K. Computational aeroacoustics: Progress on nonlinear problems of sound generation. *Progress in Aerospace Sciences*, 40(6), 345–416, August 2004.
- [19] Colonius T., Basu A. J., and Rowley C. W. Computation of sound generation and flow/acoustics instabilities in the flow past an open cavity. In *Third ASME/JSME Joint Fluids Engg Conference*, 1999.
- [20] Rowley C., Colonius T., and Basu A. On self-sustained oscillations in two-dimensional compressible flow over rectangular cavities. *J. Fluid Mechanics*, 455, 315–346, 2002.